

Capacitive Coupling And Parasitic Capacitances of Converter's – EMC

Irena KOVÁČOVÁ, Dobroslav KOVÁČ

Technical University of Košice, Slovakia

Summary: The paper is dealing with some electromagnetic compatibility (EMC) problems of converters and inverters, which are utilized for feeding of electric machines and its analyzing by PSPICE program. The main attention is focused on implications of parasitic capacitance and capacitive coupling existence.

Keywords: electromagnetic compatibility, converter, PSPICE simulation, parasitic capacitances, capacitive coupling

1. INTRODUCTION

Development of power semiconductor parts caused vehement evolution of the power electronics branch in the last fifteen years. Main focus of the above mentioned branch is concentrated to the application of individual types of power semiconductor parts in electrical circuits, which are used for electrical energy conversion of certain parameters to different parameters. Such a circuits are called converters. During the converter functionality investigation was necessary first theoretically analyze and then practically verify the assumed activity of converter. Now we can eliminate laborious theoretical analysis and economical exacting realization by numerical computer simulation, which can also disclose the startling facts concerning of the electromagnetic compatibility (EMC) problems.

2. 4Q DC IMPULSE CONVERTER AND ITS EMC

The connection of four quadrants impulse converter, which is shown in Figure 1, is usually utilized for speed DC motor regulation. Bipolar transistors and diodes are used as power semiconductor parts in this case. Each of these parts can be changed by equivalent parallel combination of its resistor and capacitor in the cut-off condition. As consequence of the fact that circuit is non-linear so the theoretical analyzing should be very difficult. If we will utilize numerical computer simulation by PSPICE program then we can do it very easy.

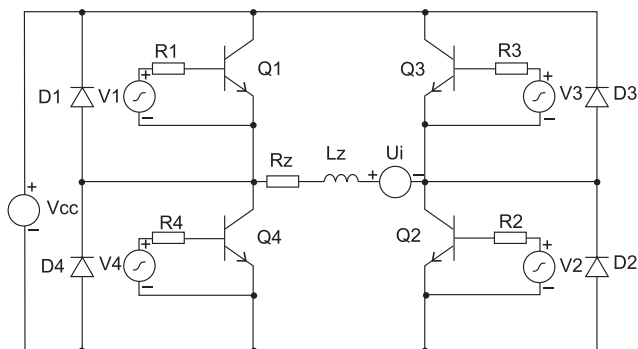


Fig. 1. 4Q DC impulse converter

First, it is necessary to write the input file with respect to the equivalent electrical scheme. After PSPICE program solving we can obtain transient curves of circuit currents and voltages. The input file example for investigated circuit is shown in following:

```
Four quadrants impulse converter
Vcc 1 0 DC 100
D1 5 1 KY195
D2 0 12 KY195
D3 12 1 KY195
D4 0 5 KY195
Q1 1 2 5 KD606
Q2 12 13 0 KD606
Q3 1 9 12 KD606
Q4 5 6 0 KD606
R1 2 3 5
R2 14 13 5
R3 10 9 5 R4 7 6 5
Rz 5 16 10
Lz 16 17 2m
Vi 17 12 DC 5
V1 3 5 PULSE(0 15 0 0 0.5m 1m)
V2 14 0 PULSE(0 15 0 0 0.5m 1m)
V3 10 12 PULSE(0 15 0.7m 0 0.3m 1m)
V4 7 0 PULSE(0 15 0.7m 0 0.3m 1m)
.MODEL KD606 NPN
.MODEL KY195 DCJO=800p
.LIB C:\SPICE1\ASIM\PARTS\NOM.LIB
.TRAN 10n 5m 0 1u
.OPTIONS ITL4=500 ITL5=0 reitl=0.01
.PROBE
.END
```

Simulation results of transistor and load currents and voltages are pictured in Figure 2. From the curves one can see that during first part of the switching period is open the first diagonal of transistors and on the rest time is open the second one. The dead time during diagonal switching is necessary from the reason of short circuit existence possibility of two transistors connected in series in one-branch. Such short circuit existence can be leading to the destruction of the both transistors. The dead time section is not visible in picture in due to existence of load inductance, which causing

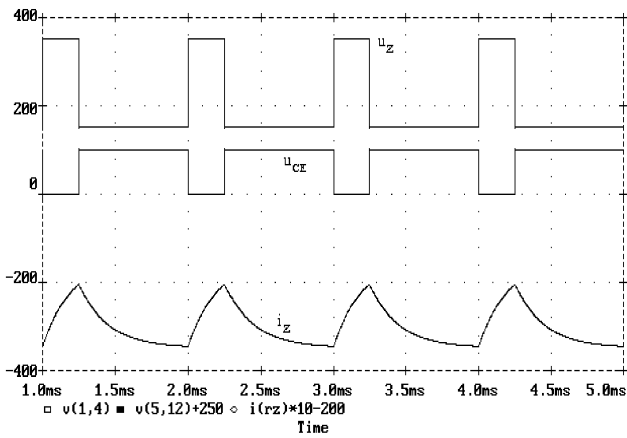


Fig. 2. Continuous current

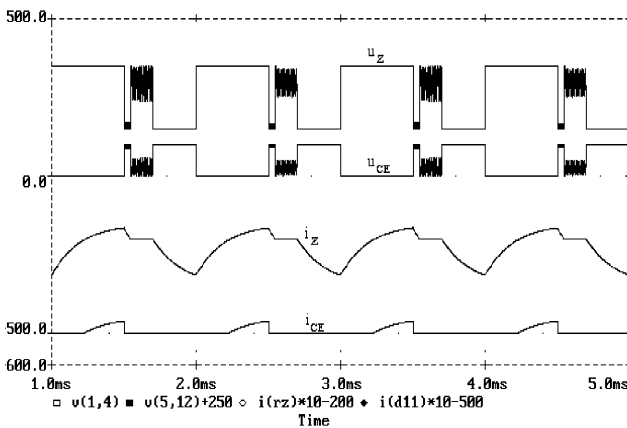


Fig. 3. Interrupted current

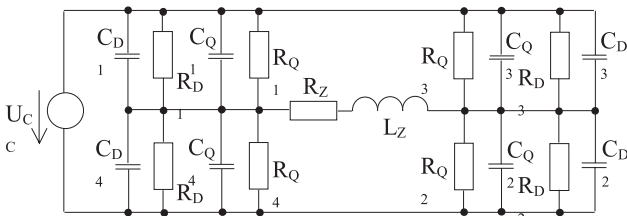


Fig. 4. Equivalent electrical scheme

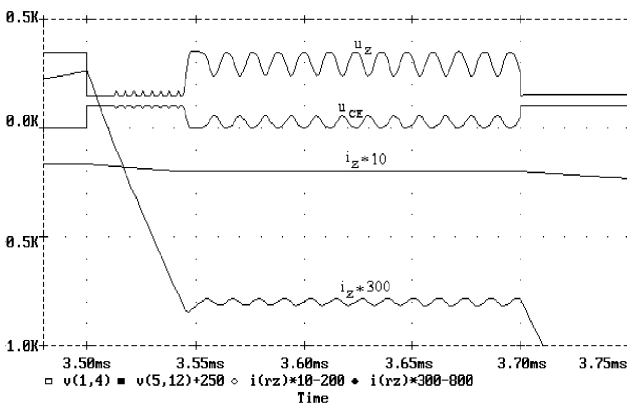


Fig. 5. Detail of oscillation process

that the current is leading through backward connected diodes and this fact exactly defines the load voltage. If we will change the ratio of the open time of the first and second diagonals in the next step, then we will change also the average value of the converter output voltage and such a way the speed of DC motor, too.

Described situation is drawing in Figure 3. From figure is evident that load current has the zero value in the particular part of period. It is resulting to the conclusion that in this time must be zeroing also load voltage by Ohm's law. However, from picture we can see that above mentioned voltage is not zero and also it is very undulating.

This fact has very unfavorable effect on the used power semiconductor parts and quality of converter electromagnetic compatibility. Simple explanation of this fact is possible to do by next figure – Figure 4, which is showing the equivalent electrical scheme of described converter at the moment when the load current is equal to zero. Each of the power semiconductor parts can be changed by equivalent parallel combination of its resistor and capacitor in the cut-off condition. $C_{Q1} = C_{Q2} = C_{Q3} = C_{Q4} = C_Q = 1200\text{pF}$, $C_{D1} = C_{D2} = C_{D3} = C_{D4} = C_D = 800\text{pF}$, $R_{Q1} = R_{Q2} = R_{Q3} = R_{Q4} = R_Q = 1330\Omega$, $R_{D1} = R_{D2} = R_{D3} = R_{D4} = R_D = 5000\Omega$, $R_Z = 10\Omega$, $L_Z = 2\text{mH}$.

Parasitic transistor and diode capacitances together with the load inductance create the resonance circuit, which is easily inclined to the oscillation. Resonant frequency is possible to state from loop impedance if its imaginary part will be equal to zero.

$$\dot{Z} = R_Z + j\omega L_Z + 2 \cdot \frac{\left(\frac{R_Q \cdot R_D}{R_Q + R_D}\right) \cdot \left(\frac{-j}{\omega \cdot (C_Q + C_D)}\right)}{\left(\frac{R_Q \cdot R_D}{R_Q + R_D}\right) + \left(\frac{-j}{\omega \cdot (C_Q + C_D)}\right)} \quad (1)$$

$$\text{Im}(\dot{Z}) = \omega L_Z - 2 \cdot \frac{\left(\frac{R_Q \cdot R_D}{R_Q + R_D}\right)^2 \cdot \left(\frac{1}{\omega \cdot (C_Q + C_D)}\right)}{\left(\frac{R_Q \cdot R_D}{R_Q + R_D}\right)^2 + \left(\frac{1}{\omega \cdot (C_Q + C_D)}\right)^2} = 0 \quad (2)$$

$$f_r = \frac{\sqrt{\frac{2}{L_Z \cdot (C_Q + C_D)} - \frac{1}{\left(\frac{R_Q \cdot R_D}{R_Q + R_D}\right)^2 \cdot (C_Q + C_D)^2}}}{2\pi} = 83272.9\text{Hz} \quad (3)$$

Detail imagination about transistor voltage, load voltage and load current, which is three hundred times magnified, we can obtain from Figure 5.

Measured waveforms are displayed in Figure 6 and Figure 7. The oscillation frequency is depending mainly on the transistor capacitance value. If the best parts with small parasitic capacitance will be used then the higher oscillation frequency and the worse EMC will be. It is evident that the

oscillation period takes $12\mu\text{s}$ and so the converter is operating as transmitter with the frequency 83.272 kHz .

3. CONVERTERS PARASITIC CAPACITANCE CALCULATION

Capacitive coupling is typical for galvanically separated circuit nodes, between which exists mutual influence by individual intensity vectors \vec{E}_i of electrostatic field, Figure 8. In such case the influence value is given by rising or decreasing slope of potential in described nodes, electrode area dimensions, space dielectric property and wire geometrical ordering in described nodes.

For predictive investigation of capacitive coupling implications we will come out from well-known Maxwell's equations valid for electrostatic field:

$$\text{rot } \vec{E} = 0 \quad (4)$$

$$\text{div } \vec{D} = \rho \quad (5)$$

where the vector of electric induction \vec{D} is given as:

$$\vec{D} = \epsilon \cdot \vec{E} \quad (6)$$

Based on physics knowledge we can state the force acting between two elementary charges Q_1 and Q_2 .

$$\vec{F} = \frac{1}{4\pi\epsilon_0} \iint_{S_1 S_2} \frac{\vec{r}_{12}}{r_{12}^3} \cdot \rho_1 \cdot dS_1 \cdot \rho_2 \cdot dS_2 \quad (7)$$

where $p_1 = dQ_1/dS_1$ and $p_2 = dQ_2/dS_2$. One element \vec{E}_{li} of electrostatic intensity vector \vec{E}_1 can be expressed as:

$$\vec{E}_{li} = \frac{\vec{F}_{li}}{Q_{2i}} = \frac{\frac{Q_{2i}}{4\pi\epsilon_0} \int_{S_1} \frac{\vec{r}_{12}}{r_{12}^3} \cdot \rho_1 \cdot dS_1}{Q_{2i}} = \frac{1}{4\pi\epsilon_0} \int_{S_1} \frac{\vec{r}_{12}}{r_{12}^3} \cdot \rho_1 \cdot dS \quad (8)$$

Total electrostatic intensity vector \vec{E} at investigated place will be given as sum of vectors \vec{E}_1 and \vec{E}_2 induced by both charged volumes. Existing voltage between these volumes is possible to express by next equation.

$$U_{12} = \varphi_1 - \varphi_2 = \int_1^2 (\vec{E}_1 + \vec{E}_2) \cdot d\vec{r}_{12} =$$

$$= \int_1^2 \left(\frac{1}{4\pi\epsilon_0} \int_{S_1} \frac{\vec{r}_{12}}{r_{12}^3} \cdot \rho_1 \cdot dS_1 + \frac{1}{4\pi\epsilon_0} \int_{S_2} \frac{\vec{r}_{21}}{r_{21}^3} \cdot \rho_2 \cdot dS_2 \right) \cdot d\vec{r}_{12} \quad (9)$$

If we will suppose that $Q_1 = Q$ and $Q_2 = -Q$, so we can write the equation for created capacitance.

$$C_{12} = \frac{Q}{U_{12}} \quad (10)$$

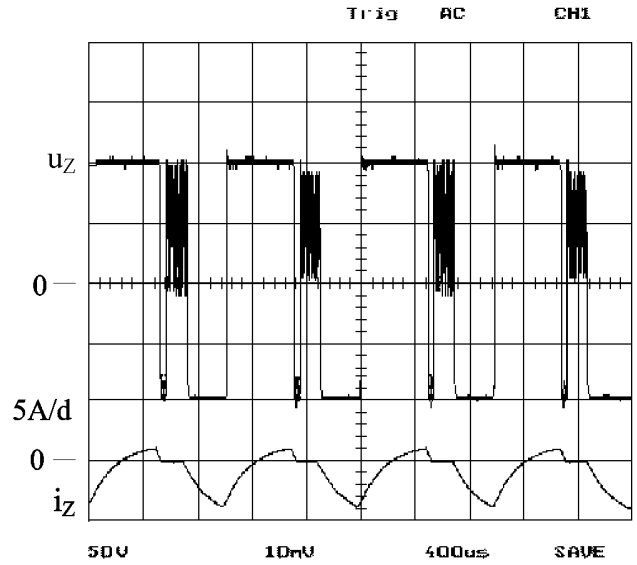


Fig. 6. Measured waveforms of load voltage u_Z and current i_Z

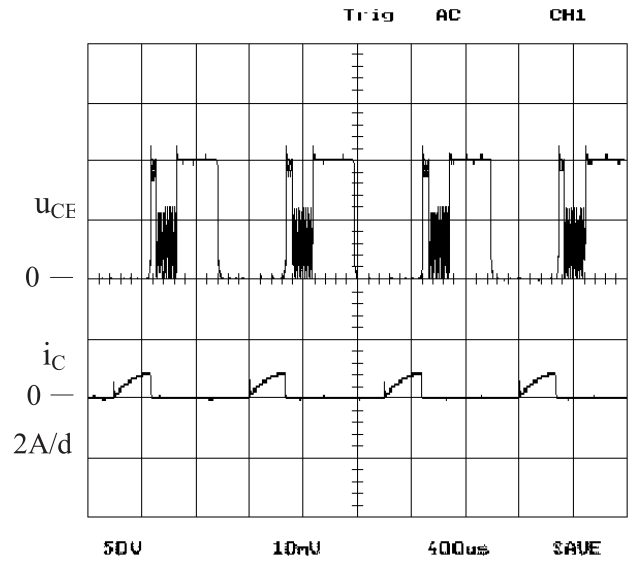


Fig. 7. Measured waveforms of transistor voltage u_{CE} and current i_C

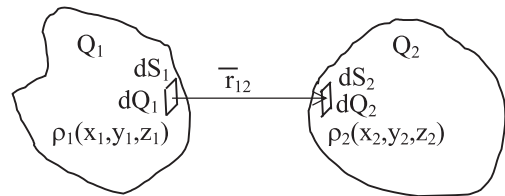


Fig. 8. Capacitive coupling

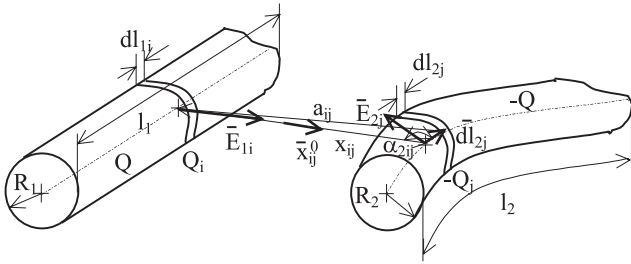


Fig. 9. Capacitive coupling

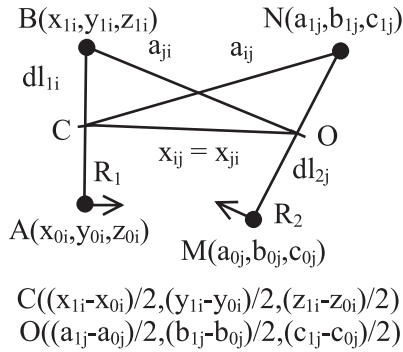


Fig. 10. 3-D Cartesian system

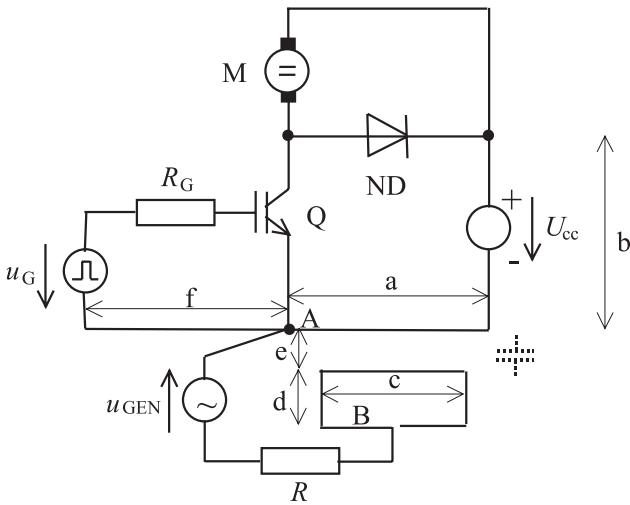


Fig. 11. Investigated circuit

are utilizing analytic-numerical method consist in differential form utilizing. For all that the following basic assumption must be done.

$$l_1 = \sum_{i=1}^{m \rightarrow \infty} dl_{1i}, \quad l_2 = \sum_{j=1}^{k \rightarrow \infty} dl_{2j} \quad (11)$$

The potential at the second wire place we can express by next equation.

$$\varphi_2 = \sum_{i=1}^m \frac{Q_i}{2\pi\epsilon dl_i} \cdot \ln \frac{x_{ij} - R_2}{R_1} \cdot \sin(\alpha_{2ij}) =$$

$$= \sum_{i=1}^m \frac{Q_i}{2\pi\epsilon dl_i} \cdot \ln \frac{x_{ij} - R_2}{R_1} \cdot \sqrt{1 - \frac{\left(x_{ij}^2 + \left(\frac{dl_{2j}}{2} \right)^2 - a_{ij}^2 \right)^2}{x_{ij} \cdot dl_{2j}}} \quad (12)$$

Similar we can state the potential for first wire position.

$$\varphi_1 = \sum_{j=1}^n \frac{-Q_j}{2\pi\epsilon dl_j} \cdot \ln \frac{x_{ji} - R_2}{R_1} \cdot \sin(\alpha_{1ji}) =$$

$$= \sum_{j=1}^n \frac{-Q_j}{2\pi\epsilon dl_j} \cdot \ln \frac{x_{ji} - R_2}{R_1} \cdot \sqrt{1 - \frac{\left(x_{ji}^2 + \left(\frac{dl_{1i}}{2} \right)^2 - a_{ji}^2 \right)^2}{x_{ji} \cdot dl_{1i}}} \quad (13)$$

Voltage between both wires will be given as:

$$U = \frac{Q}{2\pi\epsilon} \left[\sum_{i=1}^m \frac{\ln \frac{x_{ij} - R_2}{R_1} \cdot \sqrt{1 - \frac{\left(x_{ij}^2 + \left(\frac{dl_{2j}}{2} \right)^2 - a_{ij}^2 \right)^2}{x_{ij} \cdot dl_{2j}}}}{dl_{1i}} + \right.$$

$$\left. + \sum_{j=1}^n \frac{\ln \frac{x_{ji} - R_2}{R_1} \cdot \sqrt{1 - \frac{\left(x_{ji}^2 + \left(\frac{dl_{1i}}{2} \right)^2 - a_{ji}^2 \right)^2}{x_{ji} \cdot dl_{1i}}}}{dl_{2j}} \right] \quad (14)$$

Searched value of parasitic capacitance is possible to state by Coulomb's law.

$$C_{12} = \frac{2\pi\epsilon}{\sum_{i=1}^m \frac{\ln \frac{x_{ij} - R_2}{R_1} \cdot \left[1 - \frac{\left(x_{ij}^2 + \left(\frac{dl_{2j}}{2} \right)^2 - a_{ij}^2 \right)}{x_{ij} dl_{2j}} \right]}{dl_{1i}} + \sum_{j=1}^m \frac{\ln \frac{x_{ij} - R_2}{R_1} \cdot \left[1 - \frac{\left(x_{ij}^2 + \left(\frac{dl_{1j}}{2} \right)^2 - a_{ji}^2 \right)}{x_{ij} dl_{1j}} \right]}{dl_{2j}}} \quad (15)$$

Expressing of individual equation members for 3-D Cartesian system shown in Figure 10 is possible to do by the following equations.

$$dl_{1i} = \sqrt{(x_{1i} - x_{0i})^2 + (y_{1i} - y_{0i})^2 + (z_{1i} - z_{0i})^2} \quad (16)$$

$$dl_{2j} = \sqrt{(a_{1j} - a_{0j})^2 + (b_{1j} - b_{0j})^2 + (c_{1j} - c_{0j})^2} \quad (17)$$

$$a_{ij} = \sqrt{(a_{1j} - (x_{1i} - x_{0i})/2)^2 + (b_{1j} - (y_{1i} - y_{0i})/2)^2 + (c_{1j} - (z_{1i} - z_{0i})/2)^2} \quad (18)$$

$$a_{ji} = \sqrt{(x_{1i} - (a_{1j} - a_{0j})/2)^2 + (y_{1i} - (b_{1j} - b_{0j})/2)^2 + (z_{1i} - (c_{1j} - c_{0j})/2)^2} \quad (19)$$

$$x_{ij} = x_{ji} = \sqrt{\left((a_{1j} - a_{0j})/2 - (x_{1i} - x_{0i})/2 \right)^2 + \left((b_{1j} - b_{0j})/2 - (y_{1i} - y_{0i})/2 \right)^2 + \left((c_{1j} - c_{0j})/2 - (z_{1i} - z_{0i})/2 \right)^2} \quad (20)$$

Only such wire length elements dl_{1i} and dl_{2j} must be taken for total parasitic capacity calculation, which are fulfilling the next conditions.

$$x_{ji}^2 + \left(\frac{dl_{1i}}{2} \right)^2 = (x_{1i} - (a_{1j} - a_{0j})/2)^2 + (y_{1i} - (b_{1j} - b_{0j})/2)^2 + (z_{1i} - (c_{1j} - c_{0j})/2)^2 \quad (21)$$

$$x_{ij}^2 + \left(\frac{dl_{2j}}{2} \right)^2 = (a_{1j} - (x_{1i} - x_{0i})/2)^2 + (b_{1j} - (y_{1i} - y_{0i})/2)^2 + (c_{1j} - (z_{1i} - z_{0i})/2)^2 \quad (22)$$

Correctness verification of obtained results can be done by simulation and measuring. For this purpose is possible to utilize the connection of DC impulse converter shown in Figure 11.

We will try to state the value of parasitic capacitance between the node A of impulse converter and node B of sense loop. Space dielectric material is created by air. Geometrical dimensions of investigated circuits are $a = f = 0.2$ m, $b = 0.3$ m, $c = 0.1$ m, $d = 0.05$ m, $e = 0.00135$ m. Wires are made from cooper with the radius $R = 0.0006$ m. Based on above mentioned parameters it is possible to calculate the individual partial parasitic capacitances.

$$C_{ace} = \frac{1}{\frac{1}{2\pi\epsilon_0 a} \ln \frac{e-R}{R} + \frac{1}{2\pi\epsilon_0 c} \ln \frac{e-R}{R}} = 16.63 \text{ pF} \quad (23)$$

$$C_{aced} = \frac{1}{\frac{1}{2\pi\epsilon_0 a} \ln \frac{(d+e)-R}{R} + \frac{1}{2\pi\epsilon_0 (c-0.001)} \ln \frac{(d+e)-R}{R}} = 0.8306 \text{ pF} \quad (24)$$

$$C_{fce} = \frac{1}{\frac{1}{2\pi\epsilon_0 a} \ln \frac{\sqrt{e^2 + a^2} - R}{R} + \frac{1}{2\pi\epsilon_0 c} \ln \frac{\sqrt{e^2 + a^2} - R}{R}} = 0.6391 \text{ pF} \quad (25)$$

$$C_{fced} = \frac{1}{\frac{1}{2\pi\epsilon_0 a} \ln \frac{\sqrt{(d+e)^2 + a^2} - R}{R} + \frac{1}{2\pi\epsilon_0 (c-0.001)} \ln \frac{\sqrt{(d+e)^2 + a^2} - R}{R}} = 0.6314 \text{ pF} \quad (26)$$

$$C_{bdrc} = \frac{1}{\frac{1}{2\pi\epsilon_0 \frac{b}{2}} \ln \frac{\left(\sqrt{\left(\frac{b}{4} + e + \frac{d}{2} \right)^2 + \left(\frac{a}{2} + \frac{c}{2} \right)^2} - R \right)}{R} + \frac{1}{2\pi\epsilon_0 d} \ln \frac{\left(\sqrt{\left(\frac{b}{4} + e + \frac{d}{2} \right)^2 + \left(\frac{a}{2} + \frac{c}{2} \right)^2} - R \right)}{R}} = 0.3989 \text{ pF} \quad (27)$$

$$C_{bdrc} = \frac{1}{\frac{1}{2\pi\epsilon_0 \frac{b}{2}} \ln \frac{\left(\sqrt{\left(\frac{b}{4} + e + \frac{d}{2} \right)^2 + \left(\frac{a}{2} + \frac{c}{2} \right)^2} - R \right)}{R} + \frac{1}{2\pi\epsilon_0 d} \ln \frac{\left(\sqrt{\left(\frac{b}{4} + e + \frac{d}{2} \right)^2 + \left(\frac{a}{2} + \frac{c}{2} \right)^2} - R \right)}{R}} = 0.3658 \text{ pF} \quad (28)$$

$$C = C_{ace} + C_{aced} + C_{fce} + C_{fced} + 2 \cdot C_{bda-c} + 2 \cdot C_{bda+c} = 20.26 \text{ pF} \quad (29)$$

Based on calculated capacitance the simulation analyze in PSPICE program is possible to do now by circuit connection shown in Figure 12. Parameters of individual elements are $U_{CC} = 70$ V, $R_Z = 11.66 \Omega$, $L_Z = 400 \mu\text{H}$, $R = 1 \text{ M}\Omega$, $u_{\text{GEN}} = 2 \sin(\omega t)$ V. Simulation results for frequency $f = 10$ kHz are pictured in Figure 13.

The same output values obtained by simulation, but for frequency $f = 50$ kHz are shown in Figure 14. Measured values of u_{CE} , u_{GEN} and u_{C} are shown in next figures Figure 15 till to Figure 18.

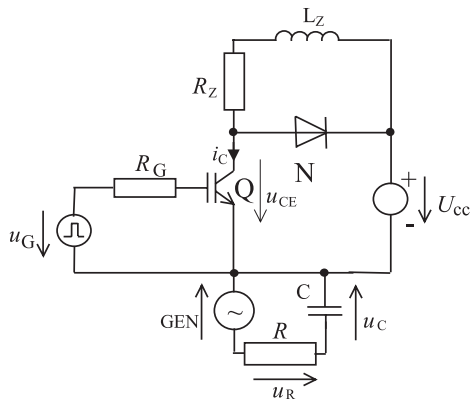


Fig. 12. Simulation circuit

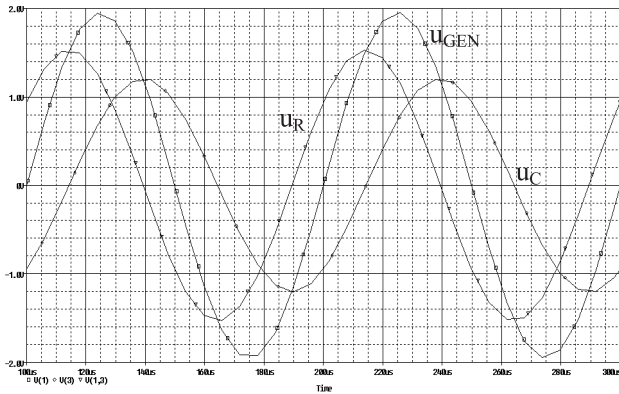


Fig. 13. Simulation results for $f = 10$ kHz

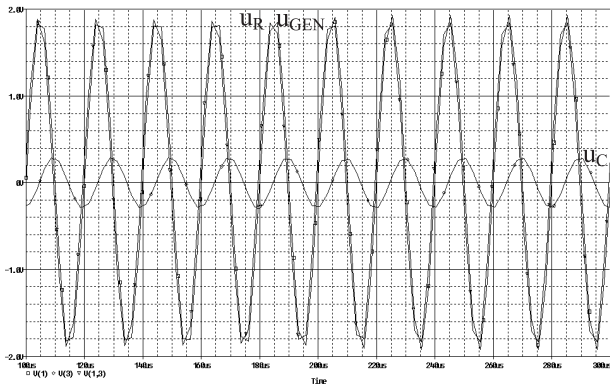


Fig. 14. Simulation results for $f = 50$ kHz

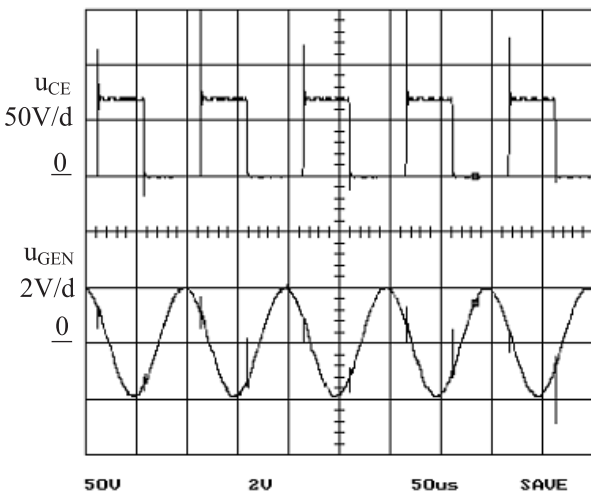


Fig. 15. Measured results for $f = 10$ kHz

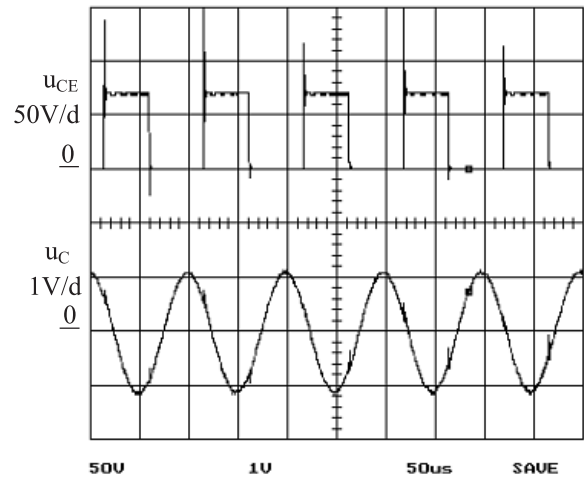


Fig. 16. Measured results for $f = 10$ kHz

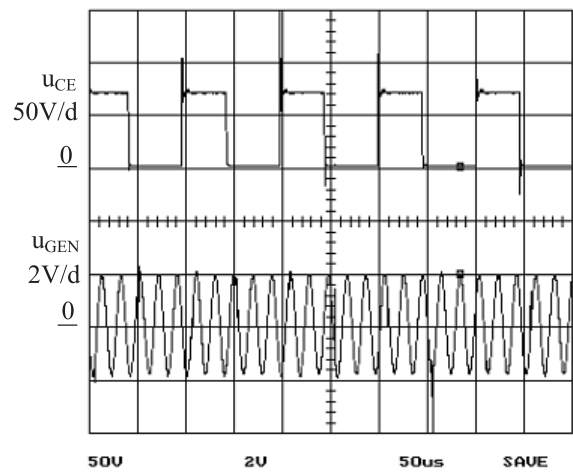


Fig. 17. Measured results for $f = 50$ kHz

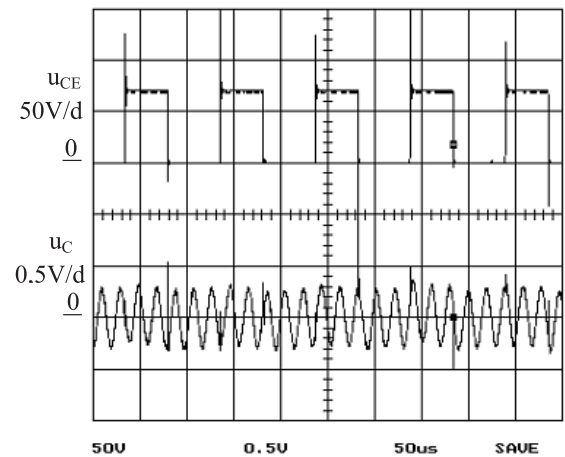


Fig. 18. Measured results for $f = 50$ kHz

By comparing of simulated and measured results one can see that obtained results are identical and it means that derived analytical formula for parasitic capacitance calculation is valid.

In due to additional verification requirement the same problem is possible to analyze also by numerical, finite element simulation method of electrostatic field. Obtained result is shown in Figure 19.

From data window is possible to state that the value of electrical flux between both nodes is $5.4357 \cdot 10^{-12}$ C. Based on the program property we must multiple this value by value of wires perimeter $l = 2 \cdot p \cdot R = 2 \cdot p \cdot 0.6 = 3.76$ mm. Total electrical flux is then 20.4382 C. In due to fact that the voltage between nodes have value 1V, so the resulting parasitic capacitance is $C = 20.4382$ pF.

By comparing of all results we can state that difference is only 0.879% and it means that the correctness of derived formula for parasitic capacitance calculation is satisfy.

4. CONCLUSION

Performed analyzes indicates that not only large current switching frequency has the main influence on the converter's EMC but equally important is also the switch off state with small parasitic resonant load current.

Obtained formula for parasitic capacitance calculation enabling predictive EMC investigation. Although such converter capacitances seem to be negligible so performed analyze show to us that it can have important influence. Mainly in the case when the switching frequency is high or one of the both nodes belong to the circuit with great impedance. It is obviously in the case of capacitive coupling existence between CMOS integrated circuits and power converter circuit when EMC quality can be very fundamental for right equipment operation.

4. ACKNOWLEDGEMENT

The paper has been prepared by support of Slovak grant project No. 1/1084/2004.

REFERENCES

1. Kaňuch, J.: *Investigation methodology design of EMC for drives with disc motor*. 2005. Dissertation thesis, FEI TU Košice.
2. Kováč, K., Lenková, A.: *Electromagnetic Compatibility*. Bratislava, 1999.
3. Carpenter, D.J.: *EMC emissions certification for large systems – a risk – management approach*. BT Technology Journal, 2003, Springer Science + Bussines Media B. V. Vol 21, No. 2, pp. 67–76.
4. *Electromagnetic compatibility*. Schaffner Elektronik GmbH, Germany, 1997.
5. Kováč, D., Kováčová, I.: *Influence of utilizing static power semiconductor converters on quality of electrical power line parameters*. Quality Innovation Prosperity, 2001, No.1, pp. 74–84.
6. Kováčová, I.: *EMC of power DC electrical drives*. Journal of Electrical Engineering, Romania, 2005, Vol. 5, No.1, pp. 61–66.
7. Šimko, V., Kováč, D., Kováčová, I.: *Bacic circuits I*. Elfa s.r.o. Publisher, 2000, 168 Pages, ISBN 80-89066-27-5.
8. Mayer, D., Ulrych, B., Škopek, M.: *Electromagnetic field analysis by modern software products*. Journal of Electrical Engineering, 2001, Vol. 7, No.1.
9. Göksu, H., Wunsh, D.C.: *Neural networks applied to electromagnetic compatibility simulations*. Lecture Notes in Computer Science, Springer - Verlag GmbH, 2003, Vol. 2714, pp. 1057–1063.

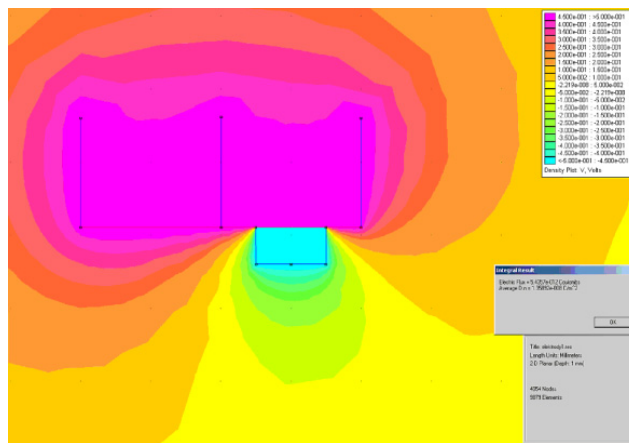


Fig. 19. Finite element method simulation

10. Rybár, R., Kudelas, D., Fischer, G.: *Alternative sources of energy III – Winding energy*. 2004, Textbook, Košice.
11. Kováčová, I., Kaňuch, J., Kováč, D.: *DC permanent magnet disc motor design with improved EMC*. Acta Technica CSAV, 2005, Vol. 50, No.3, pp. 291–306.
12. Ruddle, A.R., Parmantier, J.P., Ferrieres, X., Ward, D.D.: *Experimental validation of time – domain electromagnetic models for field coupling into the interior of a vehicle from a nearby broadband antenna*. Proceedings of IEE International Conference on Communication in Electromagnetic GEM 2004, Stratford-Upon-Avon, pp. 133–134.
13. Gallová, Š.: *A Progressive manufacturing operation*. International Congress MATAR. Prague, 2004, pp. 141–146.
14. Kováčová, I., Kováč, D.: *Converter's EMC – parasitic capacitances*. Electronics Letters, 2005, Vol. 5, No.1, pages 6, ElectronicsLetters.com, ISSN 1213-161X
15. Kováčová, I., Kaňuch, J., Kováč, D.: *EMC power electrotechnics systems*. Equilibria Publisher, 2005, s.r.o., Košice, 182 pages.
16. Kováčová, I., Kováč, D.: *EMC compatibility of power semiconductor converters and inverters*. Acta Electrotechnica et Informatica, 2003, No.2, Vol. 3, pp. 12–14.
17. Kováč, D.: *Simulation models of power elements in PSpice program*. Proceedings of Conference on Power Electronics and Motion Control, 1994, PEMC'94, Warsaw.
18. Kováčová, I., Kováč, D.: *Safeguard circuits of power semiconductor parts*. Acta Electrotechnica et Informatica, 2003, No.3, Vol. 3, pp. 44–45.
19. Kůs, V.: *The influence of power semiconductor converters on power distribution net*. BEN – technical literature Publisher, Praha, 2002, 184 pages.
20. Novák, P., Babarík, P., Janoščík, J.: *Surface effects impact on conductor impedance*. Electrical Power Quality and Utilisation, 2003, No. 1, Vol. 9, pp. 75–80.



Irena Kováčová (Assoc. Prof., CSc.)

Born in 1958. She finished her studies in 1982 at the Technical University of Košice, Department of Electrical Drives, direction — Power electronics with excellent evaluation. From this time she has worked at the Department of Electrical Drives, first as assistant lecturer and now as associate professor. In 1988 she has got her doctoral diploma. In 1991 she has got the Award of Minister of Education for

Development of Science and Technology. Her working interest is mainly focused to the field of power electronics, especially to the construction of converters and inverters with new perspective elements and computer simulation of new power semiconductor parts and devices.

Address:

Department of Electrical Drives and Mechatronics,
 Technical University of Košice,
 Letná 9, 042 00 Košice, Slovak Republic,
 E-mail: Irena.Kovacova@tuke.sk



Dobroslav Kováč (Prof., CSc.)

Born in 1961. He finished his studies in 1985 at the Technical University of Košice, Department of Electrical Drives, direction — Power electronics with excellent evaluation. Then he worked as research worker at the Department of Electrical Drives. His research work was focused to the practical application of new power semiconductor devices. In 1989 he has got the Award of Minister of Education for Development of Science and Technology. From 1991 he has worked as assistant lecturer at the Department of Theoretical electrical engineering and Electrical measurement. He got his doctoral diploma in 1992 for the work on the field of power electronics. From 2000 he worked as professor and his working interest is now focused mainly to the field of computer simulation of power electronic circuits and automated computer measuring. From 1999 he is also working as Vice-dean of faculty.

Address:

Department of Theoretical Electrical Engineering and Electrical Measurement,

Park Komenského 3, 042 00 Košice, Slovak Republic,

phone: (+421) 602 2516, (+421) 602 20 24,

E-mail: Dobroslav.Kovac@tuke.sk